

# Antibody-Dependent Effector Functions Against HIV Decline in Subjects Receiving Antiretroviral Therapy

Vijaya Madhavi,<sup>1</sup> Fernanda E. Ana-Sosa-Batiz,<sup>1</sup> Sinthujan Jegaskanda,<sup>1</sup> Rob J. Center,<sup>1,b</sup> Wendy R. Winnall,<sup>1</sup> Matthew S. Parsons,<sup>1</sup> Jintanat Ananworanich,<sup>3</sup> David A. Cooper,<sup>2</sup> Anthony D. Kelleher,<sup>2</sup> Denise Hsu,<sup>2</sup> Sarah Pett,<sup>2,4</sup> Ivan Stratov,<sup>1</sup> Marit Kramski,<sup>1,a</sup> and Stephen J. Kent<sup>1,a</sup>

<sup>1</sup>Department of Microbiology and Immunology, Peter Doherty Institute for Infection and Immunity, University of Melbourne, Parkville, and <sup>2</sup>Kirby Institute for Infection and Immunity in Society, University of New South Wales, Sydney, Australia; <sup>3</sup>Thai Red Cross AIDS Research Centre, HIV Netherlands Australia Thailand Research Collaboration, Bangkok, Thailand; and <sup>4</sup>Medical Research Council Clinical Trials Unit, Department of Infection and Population Health, University College London, United Kingdom

**Background.** Combination antiretroviral therapy (cART) effectively controls human immunodeficiency virus (HIV) infection but does not eliminate HIV, and lifelong treatment is therefore required. HIV-specific cytotoxic T lymphocyte (CTL) responses decline following cART initiation. Alterations in other HIV-specific immune responses that may assist in eliminating latent HIV infection, specifically antibody-dependent cellular cytotoxicity (ADCC) and antibody-dependent phagocytosis (ADP), are unclear.

**Methods.** A cohort of 49 cART-naïve HIV-infected subjects from Thailand (mean baseline CD4 count, 188 cells/ $\mu$ L; mean viral load, 5.4 log<sub>10</sub> copies/mL) was followed for 96 weeks after initiating cART. ADCC and ADP assays were performed using serum samples obtained at baseline and after 96 weeks of cART.

**Results.** A 35% reduction in HIV type 1 envelope (Env)-specific ADCC-mediated killing of target cells ( $P < .001$ ) was observed after 96 weeks of cART. This was corroborated by a significant reduction in the ability of Env-specific ADCC antibodies to activate natural killer cells ( $P < .001$ ). Significantly reduced ADP was also observed after 96 weeks of cART ( $P = .018$ ).

**Conclusions.** This longitudinal study showed that cART resulted in significant reductions of HIV-specific effector antibody responses, including ADCC and ADP. Therapeutic vaccines or other immunomodulatory approaches may be required to improve antibody-mediated control of HIV during cART.

**Keywords.** HIV; cART; ADCC; ADP; monocytes; NK cells.

Combination antiretroviral therapy (cART) has improved the health and prolonged the life of human immunodeficiency virus (HIV)-infected individuals. cART results in an increase in the number of CD4 T cells and a reduction in viral load but does not eliminate

latent reservoirs [1–3]. Clinical trials attempting to purge latent HIV-infected cells by virus activation from latency to achieve a cure for HIV are currently underway [4, 5]. If not eliminated, reactivated latently infected cells could return into the latent state. There is increasing interest in the modulation of HIV immunity to achieve improved control of viremia in the absence of cART [1, 6].

HIV-specific cytotoxic T lymphocyte (CTL) responses decline in HIV-infected individuals during cART [7]. Although CTL responses are likely to be important in the clearance of latently infected cells [8], it is difficult to induce protective anti-HIV CTLs with current vaccine strategies [9, 10]. Levels of antibodies (Abs) specific for HIV, as another arm of the adaptive immune response to the virus, also decline in patients during cART [11–13]. The decline in total Ab levels seen in the apparently successfully cured so-called Berlin

Received 15 April 2014; accepted 12 August 2014; electronically published 28 August 2014.

Presented in part: AIDS Vaccine 2013, Barcelona, Spain, 7–10 October 2013.

<sup>a</sup>M. K. and S. J. K. contributed equally to this report.

<sup>b</sup>Present affiliation: Burnet Institute, Melbourne, Australia.

Correspondence: Stephen J. Kent, MD, Department of Microbiology and Immunology, The University of Melbourne at the Peter Doherty Institute for Infection and Immunity, Parkville, Victoria 3010, Australia (skent@unimelb.edu.au).

The Journal of Infectious Diseases® 2015;211:529–38

© The Author 2014. Published by Oxford University Press on behalf of the Infectious Diseases Society of America. All rights reserved. For Permissions, please e-mail: journals.permissions@oup.com.

DOI: 10.1093/infdis/jiu486

patient suggests that the reduction in antigen load leads to the eventual decline of Ab levels [1, 14].

The effect of cART on Abs with Fc-mediated functional capacities, including Ab-dependent cellular cytotoxicity (ADCC) and Ab-dependent phagocytosis (ADP), has not been reported. ADCC Abs bind to viral antigens on the surface of infected cells and, via Fc receptor, recruit and activate innate immune cells such as natural killer (NK) cells and monocytes to secrete cytokines and chemokines to kill the infected cell. The importance of Fc-mediated functions was recently highlighted by the partially successful RV144 HIV vaccine trial, in which ADCC Abs were associated with protection from HIV [15, 16]. The potential role of ADCC in protection from infection and slower disease progression has also been highlighted in various studies [17–20].

ADP is another potentially important Ab effector function that can eliminate anti-HIV Ab-opsonized complexes through Fc $\gamma$  receptors (Fc $\gamma$ R) expressed on monocytes and macrophages [21]. Recent studies suggest a role for ADP in the protection of macaques from simian/human immunodeficiency virus (SHIV) and control of disease [22–24].

We hypothesized that ADCC and ADP Ab levels decline during cART if viral loads are suppressed, since less viral antigen is available to stimulate ADCC and ADP Ab production. We found that both ADCC and ADP decline substantially after 2 years of cART.

## MATERIALS AND METHODS

### Study Subjects

Forty-nine initially cART-naive HIV-infected subjects from Thailand were studied before and during cART (Table 1). The mean age of the subjects was 32 years (range, 20–51 years). All participants were enrolled in the RESTORE study [25, 26] and consented to donating blood specimens. HIV-negative volunteers provided effector peripheral blood mononuclear cells (PBMCs) for the assays conducted. The study was performed under the auspices of the Alfred Human Health Research and Ethics Committee (Melbourne, Australia) and the Chulalongkorn University Institutional Review Board (Bangkok, Thailand).

### Purification of Immunoglobulin G (IgG) From Patient Serum

Total IgG was purified from 50 to 100  $\mu$ L of patient sera, using the Protein G HP Multitrap and the Antibody Buffer Kit (both from GE Healthcare, Uppsala, Sweden). Elution was repeated 2 times, and pooled elutes were washed twice with phosphate-buffered saline (PBS). IgG concentration was determined using the NanoDrop 2000.

### HIV Type 1 (HIV-1) Antigens

HIV-1<sub>93TH966</sub> gp140 Env (subtype AE) protein and a control simian immunodeficiency virus (SIV)<sub>MAC239</sub> gp140 protein were produced from stable Env-expressing HeLa cell lines, using previously published techniques [27]. Briefly, Env was purified from conditioned medium (serum-free Optimem, Life Technologies), using lentil lectin affinity chromatography and size exclusion chromatography, with Superdex 200 (GE Healthcare) as resin. Fractions containing Env oligomers (enriched for Env trimers) [28] were pooled, concentrated, and stored at 4°C until used. Fifteen amino acid-long peptides overlapping by 11 amino acids were constructed spanning the HIV-1 subtype AE CD4 binding site-deleted Env (164 peptides); Auspep, Parkville, Australia) [29]. The CD4 binding site sequence was reconstituted by adding the corresponding peptides from the HIV-1 subtype B (National Institutes of Health AIDS reagent repository catalog no. 6451). All peptides solubilized in dimethyl sulfoxide and pooled to a single pool spanning the complete Env protein.

### Anti-Env IgG Enzyme-Linked Immunosorbent Assay (ELISA)

Gp140-specific serum IgG binding titers were measured by ELISA as previously described [30]. Briefly, purified HIV-1<sub>93TH966</sub> gp140 Env (subtype AE) in coating buffer (20 mM Tris [pH 8.8] and 100 mM NaCl) was coated onto 96-well flat-bottomed plates at 100 ng/well overnight. After blocking with 5% skim milk powder for 1 hour, sera were added in a half-log<sub>10</sub> (3.16-fold) dilution series. After 4 hours of incubation, horseradish peroxidase-conjugated rabbit anti-human IgG Ab (Sigma) was added, and specimens were incubated for 1 hour. Color reactions were developed using 3,3'-5,5'-tetramethylbenzidine, and absorbance was measured at 450 nm against a reference of OD of 492 nm. A positive signal was defined as

**Table 1. Cohort Characteristics, by Time After Combination Antiretroviral Therapy Initiation**

Characteristic	Week 0	Week 4	Week 8	Week 12	Week 24	Week 48	Week 96
CD4 count, cells/ $\mu$ L							
Mean	188	265	298	296	307	361	401
Range	10–424	28–584	51–660	64–650	78–729	85–795	114–990
HIV load, copies/mL							
Mean	244 682	1576	609	1300	513	755	46
Range	815–1 969 218	40–51 308	40–15 138	40–57 127	40–22 849	40–34 905	40–137
Undetectable HIV load, patients, no.	0	3	15	25	44	44	44

Abbreviation: HIV, human immunodeficiency virus.

one giving an OD at least 3-fold higher than that obtained with HIV-negative sera.

### Rapid Fluorometric ADCC Assay

The rapid fluorometric ADCC assay is a killing-based assay of ADCC immunity and was performed as previously described [31, 32]. Briefly,  $1 \times 10^6$  CEM.NKr-CCR5 cells were coated with 3  $\mu$ g of purified HIV-1<sub>93TH966</sub> gp140 Env (subtype AE) and a control SIV<sub>MAC239</sub> gp140 protein separately for 1 hour at room temperature. Gp140-coated and -uncoated CEM.NKr-CCR5 cells were subsequently labeled with PKH26 and CFSE (both Sigma) according to the manufacturer's instructions. PKH26<sup>+</sup>CFSE<sup>+</sup>-labeled CEM.NKr-CCR5 target cells were opsonized with serum or purified IgG from HIV-1-infected individuals for 30 minutes at 37°C. PBMCs from a healthy donor were added to target cells at a target to effector cell ratio of 1:10. After 4 hours of incubation at 37°C, cells were stained for CD3 (anti-human CD3-PerCp, BD Biosciences, clone SK7) and CD14 (anti-human CD14-APC-H7, BD Biosciences, clone MØP9) for 30 minutes at room temperature. Cells were fixed and analyzed using a FACS-LSR II cytometer and FlowJo analysis software (version 9.4.9.). The readout is performed by gating on CFSE<sup>-</sup>CD14<sup>+</sup> monocytes that acquire the target cell PKH26 dye as a result of ADCC-mediated killing. The rapid fluorometric ADCC assays had low mean background responses ( $\pm$ standard error of the mean [SEM]) to no antigen stimulation ( $3.7\% \pm 0.3\%$  and  $5.0\% \pm 0.8\%$  at weeks 0 and 96, respectively) that were similar to responses to the irrelevant SIV gp140 control protein ( $4.4\% \pm 0.4\%$  and  $6.2\% \pm 1.1\%$  at weeks 0 and 96, respectively).

### ADCC-Mediated NK Cell Activation Assay

The whole blood-based NK cell activation ADCC assay was used to analyze intracellular cytokine expression and degranulation of ADCC-activated NK cells as described previously [33, 34]. In brief, 150  $\mu$ L of HIV-negative donor blood in sodium heparin anticoagulant, 5  $\mu$ L of HIV-positive subject sera, HIV-1 Env (subtype AE) peptide pool (1  $\mu$ g/mL final concentration), brefeldin A (10  $\mu$ g/mL final concentration, Sigma), monensin (10  $\mu$ g/mL final concentration; BD Biosciences), and APC-H7-conjugated anti-CD107a Ab (clone H4A3; Biolegend) were mixed together and incubated at 37°C for 5 hours, followed by surface staining with anti-human CD3 PerCP (clone SK7; Biolegend) and anti-human CD56 PE-Cy7 (clone HCD56; Biolegend) Abs. Next, red blood cells were lysed with FACS Lyse (BD Biosciences), and remaining white blood cells were permeabilized with FACS Perm-2 solution (BD Biosciences) before staining with anti-human interferon  $\gamma$  (IFN- $\gamma$ )-APC Ab (clone B27; Biolegend). Cells were fixed and analyzed using a FACS-LSR II cytometer and FlowJo analysis software (version 10.0.6). NK cells were identified as

CD3<sup>-</sup>CD56<sup>+</sup> cells, and ADCC responses were measured as the percentage of NK cells expressing IFN- $\gamma$  and CD107a. The responses were considered positive if the response positive for CD107a and IFN- $\gamma$  was  $>3$  times that for unstimulated NK cells in the absence of Env peptides but in the presence of subject sera.

### Ab-Dependent Phagocytosis (ADP) Assay

Based on the standard HIV-specific ADP assay [35], a modified ADP assay was developed to measure internalization of HIV Ab-opsonized targets, using a specific hybridization internalization probe [36, 37]. Three microliters of FITC-labeled NeutrAvidin FluoroSpheres (bead diameter, 1  $\mu$ m; Invitrogen) were coated with 0.75  $\mu$ g HIV-1<sub>93TH966</sub> gp140 Env and a control SIV<sub>MAC239</sub> gp140 protein separately with 3  $\mu$ L of 150  $\mu$ M biotin- and Cy5-labeled fluorescent internalization probe (5'-Cy5-TCAGTTCAGGACCCTCGGCT-N3-3'; Integrated DNA Technologies) and incubated overnight at 4°C [36]. Beads were washed to remove unbound gp140 and the Cy5-labeled fluorescent internalization probe. Ten microliters of a 1:10 dilution of coated beads were opsonized with HIV-infected serum-purified IgG (1  $\mu$ g/mL final concentration) for 2 hours at 37°C and then incubated with  $1 \times 10^5$  THP1 cells (a monocytic cell line) in a total volume of 200  $\mu$ L for 16 hours at 37°C. Surface-bound beads were quenched by adding 1  $\mu$ g/ $\mu$ L of the complementary quenching DNA probe (5'-AGCCGAGGGTCCTGAAGTGA-BHQ2-3'; Integrated DNA Technologies) and incubated for 10 minutes at 4°C [36]. Cells were fixed and analyzed using a FACS-LSR II cytometer and FlowJo analysis software (version 9.6.2). Mean background uptake ( $\pm$ SEM) of beads coated with the control SIVgp140 protein was not different between IgG samples collected during weeks 0 and 96 after cART initiation ( $11.2\% \pm 0.3\%$  and  $11.5\% \pm 0.1\%$  at weeks 0 and 96, respectively). Background levels of uptake of the control SIVgp140-coated beads were similar to uptake of uncoated beads without IgG (9.9%) or HIV-1 gp140-coated beads using IgG from a HIV negative donor (12.4%).

### Monocyte Phenotype and Fc $\gamma$ R Expression

We evaluated percentages of monocyte subsets and Fc receptor expression using frozen PBMCs collected at baseline and after 96 weeks of cART. Cells were thawed, washed twice with RF10 medium (consisting of Roswell Park Memorial Institute 1640 medium [Invitrogen Life Technologies] supplemented with 10% fetal calf serum, 1% penicillin-streptomycin, and 2% glutamine), and washed with PBS containing 2 mM ethylenediaminetetraacetic acid (EDTA). Live/Dead Aqua dead cell stain (Life Technologies) was added to cells for 20 minutes and washed with PBS containing 2 mM EDTA. Cells were resuspended in RF10 medium and stained with anti-human CD3 PerCp (clone SK7; BD Biosciences), anti-human CD32 APC (clone FLI8.26; BD Biosciences), anti-human CD14 APCH7

(clone MøP9; BD Biosciences), anti-human CD16 FITC (clone 3G8; BD Biosciences), and anti-human CD64 PECy7 (clone 10.1; BD Biosciences) Abs for 30 minutes at room temperature. Cells were then washed with PBS containing 0.5% (w/v) bovine serum albumin (Sigma-Aldrich) and 2 mM EDTA and fixed in 1% (v/v) formaldehyde.

### Statistical Analyses

Statistical analyses were performed using GraphPad Prism, version 6.0 (GraphPad Software, San Diego, California), and SPSS software, version 18 (IBM, Armonk, New York). Data were analyzed by the paired *t* test to compare means (Figure 1B and 1C, Figure 2B and 2C, Figure 3B, and Figure 4B, 4C, and 4D) and by repeated-measures 1-way analysis of variance together with the Tukey post-hoc test to compare means (Figure 1D). A Wilcoxon signed rank test was used where the sample size was low (Figure 2D). An  $\alpha$  level of 0.05 was considered to indicate a significant difference. Each assay (the rapid fluorometric ADCC, ADCC-mediated NK cell activation, and ADP assays) was replicated at least twice in independent experiments to validate any differences after cART initiation.

## RESULTS

### Reduced Total Env-Specific Abs After Long-term cART

Previous studies suggest that long-term cART reduces Env-specific total and neutralizing Abs [11–13], although the effect of cART on Abs with other effector functions is not known. To confirm previous findings on the total Env-specific Ab response with our cohort of 49 HIV-infected Thai subjects, we determined gp140-specific serum end point titers at baseline and after 96 weeks of cART. The mean  $\log_{10}$  end point titer ( $\pm$ SEM) was significantly reduced from week 0 ( $4.65 \pm 0.084$ ) to week 96 ( $3.95 \pm 0.12$ ;  $P < .001$ ).

### Reduced HIV-Specific ADCC-Mediated Killing Following Long-term cART

Since total Env Abs and other HIV-specific immune responses, such as CTL responses, decline during long-term cART [7, 11–13], we hypothesized that Env-specific ADCC would also decline. We first studied the effect of cART on ADCC Ab-mediated killing, using the rapid fluorometric ADCC assay. The rapid fluorometric ADCC assay is a killing-based

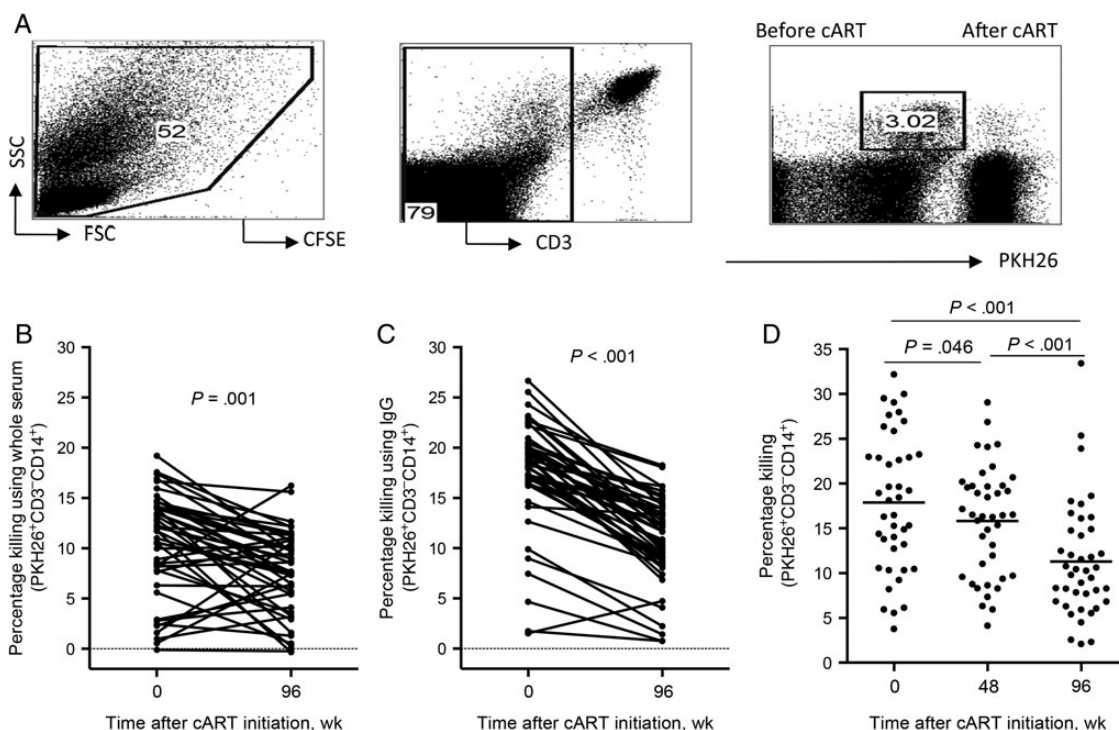


**Figure 1.** Reduced human immunodeficiency virus (HIV)-specific antibody-dependent cellular cytotoxicity (ADCC)-mediated killing following long-term combination antiretroviral therapy (cART). *A*, Gating on CFSE<sup>+</sup> cells followed by gating on CD3<sup>+</sup>CD14<sup>+</sup> monocytes and analysis of PKH26 expression on monocytes. A side-by-side comparison of PKH26 expression for serum samples obtained before and after cART initiation from 1 subject. *B*, ADCC-mediated killing of target cells coated with HIV type 1 (HIV-1)<sub>93TH966</sub> gp140 subtype AE, using 49 subjects' serum samples from weeks 0 and 96 of cART. The dotted line indicates percentage killing for a HIV-negative serum. *C*, ADCC-mediated killing performed on serum-purified immunoglobulin G (IgG) from all 49 subjects to HIV-1<sub>93TH966</sub> gp140 subtype AE. The dotted line indicates percentage killing for a HIV-negative serum purified IgG. For data represented in panels *B* and *C*, means were compared using paired *t* tests. *D*, The kinetics of ADCC-mediated killing for 41 subjects at weeks 0, 48, and 96 after cART. Comparisons were made using repeated-measures 1-way analysis of variance and the Tukey post-hoc test. Lines in the graph represent mean bars.

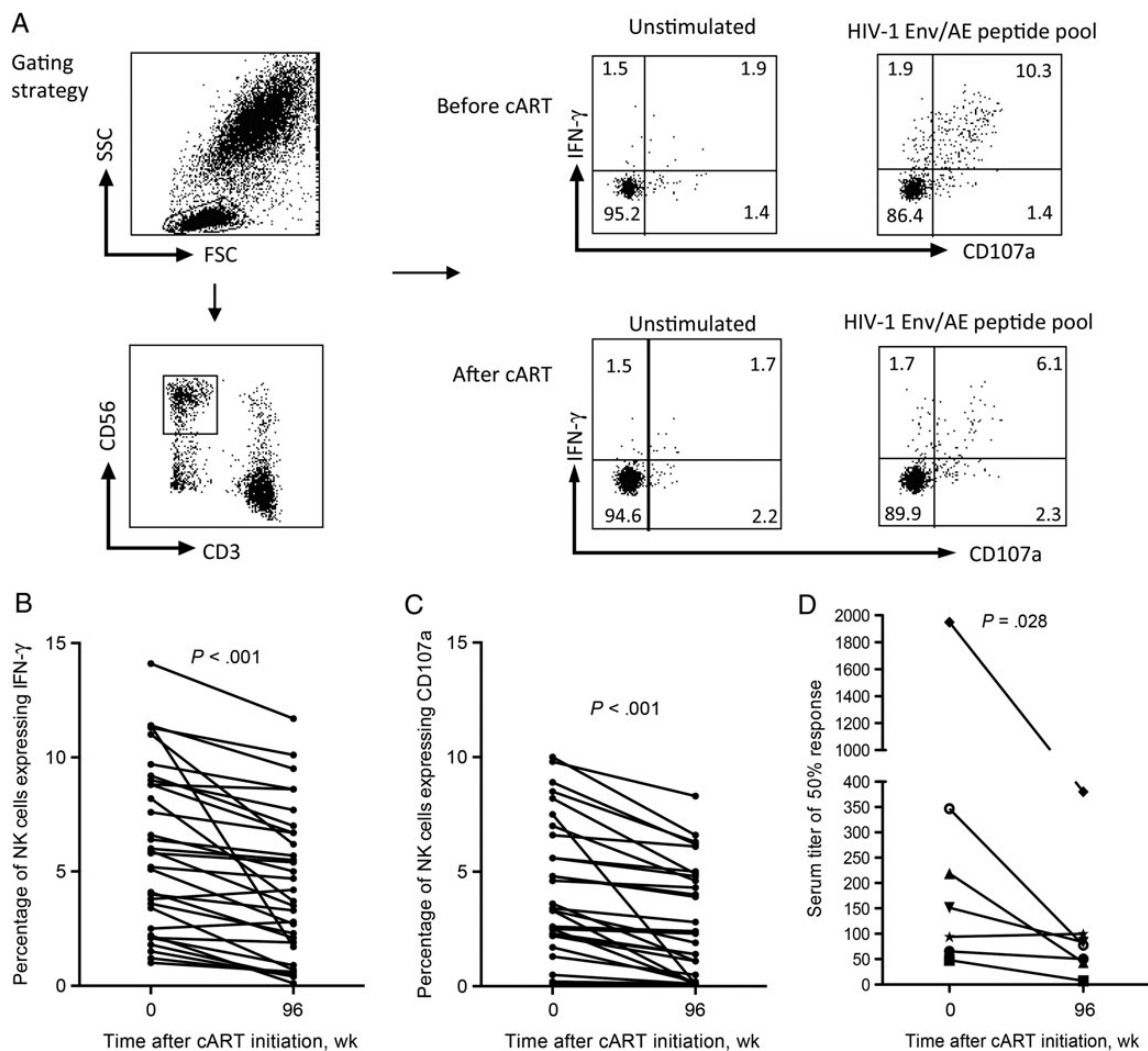


**Figure 2.** Decreased human immunodeficiency virus (HIV)-specific antibody (Ab)-mediated natural killer (NK) cell activation following long-term combination antiretroviral therapy (cART). *A*, Gating strategy for the HIV-specific Ab-mediated NK cell activation assay. First gate is on lymphocytes in the forward and side scatter (FSC/SSC) plot and then on CD3<sup>+</sup>CD56<sup>+</sup> NK cells, which are analyzed for total intracellular interferon  $\gamma$  (IFN- $\gamma$ ) and total CD107a expression. A flow cytometric example of pre-cART and post-cART Ab-dependent cellular cytotoxicity (ADCC) responses to HIV-1 Env/AE peptide pool, compared with unstimulated control (presence of HIV-positive sera but absence of peptide) is shown (values represent the percentage of NK cells expressing IFN- $\gamma$  and CD107a). *B* and *C*, Serum samples from all 49 subjects analyzed for the percentage of NK cells expressing IFN- $\gamma$  (*B*) and CD107a (*C*) from baseline (week 0) and 96 weeks after initiation of cART. For data represented in panels *B* and *C*, means were compared using paired *t* tests. *D*, ADCC Ab titers for 7 randomly selected subjects and half-log dilution of the week 0 and week 96 serum samples tested with the NK cell activation assay. Comparisons were made using the Wilcoxon signed rank test.

ADCC assay that measures the loss of integrity of gp140-coated target cells. Figure 1A shows the rapid fluorometric ADCC assay gating strategy and an example for responses at baseline (week 0) and after week 96 of cART. We tested sera from 49 subjects at baseline and 96 weeks after commencement of cART and found that mean Ab-mediated killing ( $\pm$ SEM) significantly declined from baseline ( $10.3\% \pm 0.8\%$ ) to week 96 ( $7.1\% \pm 0.7\%$ ;  $P = .001$ ; Figure 1B). To validate that killing was Ab-mediated and not due to target cell activation by other factors in the sera (such as cytokines), IgG from subject's sera were purified

and retested in the rapid fluorometric ADCC assay. Using the purified IgG samples in the rapid fluorometric ADCC assay, we confirmed that the killing was mediated by IgG and that mean Ab-mediated target cell killing ( $\pm$ SEM) decreased from baseline ( $17.6\% \pm 0.8\%$ ) to week 96 after cART initiation ( $10.9\% \pm 0.6\%$ ;  $P < .001$ ; Figure 1C).

To investigate the timing of the decline of ADCC Abs during long-term cART, we tested 41 of 49 subjects from whom sufficient serum specimens were available at weeks 0, 48, and 96 after cART initiation. We found a small but significant

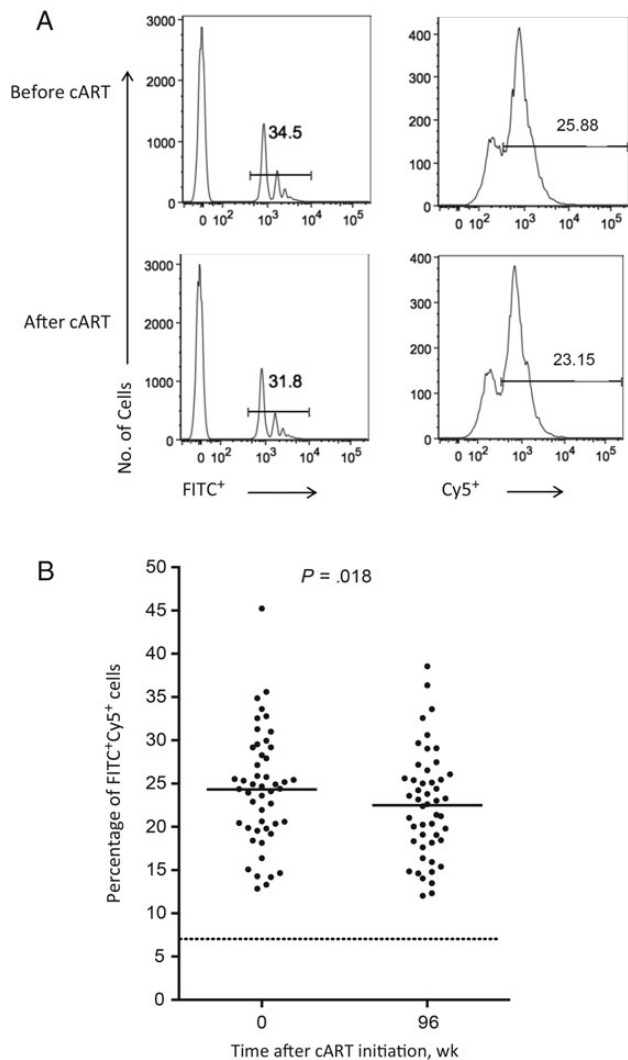


**Figure 3.** Reduced human immunodeficiency virus (HIV)-specific antibody (Ab)-dependent phagocytosis (ADP) following long-term combination antiretroviral therapy (cART). *A*, Gating strategy for the ADP assay. Cells with at least 1 bead (FITC<sup>+</sup>) were assessed for their Cy5 fluorescence (Cy5<sup>+</sup>; internalized beads). *B*, ADP was determined for serum-purified immunoglobulin G (IgG) from all 49 subjects at week 0 and week 96 after commencement of cART. ADP was measured against HIV type 1 (HIV-1)<sub>93TH966</sub> gp140 subtype AE. The dotted line indicates percentage phagocytosis in presence of HIV-negative IgG pool. Comparisons were made using paired *t* tests. Lines in the graph represent mean bars.

reduction ( $\pm$ SEM) in mean ADCC activity ( $\pm$ SEM) in serum samples from week 0 ( $17.9\% \pm 1.2\%$ ) to week 48 ( $15.8\% \pm 0.9\%$ ;  $P = .046$ ; Figure 1*D*) of cART. There was a larger drop in mean ADCC activity ( $\pm$ SEM) from week 48 to week 96 ( $11.3\% \pm 1.0\%$ ;  $P < .001$ ; Figure 1*D*).

### Reduced HIV-Specific ADCC-Mediated NK Cell Activation Following Long-term cART

The process of ADCC results not only in the killing of the target cell, but also in the activation of NK cells to express a variety of

antiviral cytokines, including IFN- $\gamma$ . To confirm and expand the results of the rapid fluorometric ADCC assay described above, we tested all sera from all 49 subject for the ability to induce ADCC-mediated NK cell activation, comparing baseline values (week 0) and week 96 values obtained using the ADCC Ab-mediated peptide-based NK cell activation assay. This assay measures Ab-dependent NK cell degranulation (CD107a surface expression) and intracellular expression of IFN- $\gamma$  [33, 34]. The gating strategy for this assay is shown in Figure 2*A*. We found that long-term cART resulted in a significant reduction in both mean ( $\pm$ SEM) Ab-mediated NK cell IFN- $\gamma$  expression (from  $6.1\% \pm 0.7\%$  at week 0 to  $4.0\% \pm 0.6\%$  at week 96;  $P < .001$ ; Figure 2*B*) and CD107a degranulation (from  $3.9\% \pm 0.5\%$  at week 0 to  $2.5\% \pm 0.4\%$  at week 96;  $P < .001$ ; Figure 2*C*). To determine the magnitude of the reduction in ADCC Ab titers, we randomly selected 7 subjects and tested the half-log<sub>10</sub> dilution (3.16-fold) of the week 0 and week 96 serum samples. We detected a median 1.9-fold reduction in ADCC Ab-mediated NK cell activation (as measured by IFN- $\gamma$ <sup>+</sup> and CD107a<sup>+</sup> double-positive NK cells) from baseline (median, 151.4 [IQR, 281]) to week 96 of cART (median, 77.6 [IQR, 56.4];  $P = .028$ , by the Wilcoxon signed rank test; Figure 2*D*).

### Reduced Env-Specific Ab-Dependent Phagocytosis Following Long-term cART

Nonneutralizing Ab responses such as HIV-specific ADP may assist in immunity to HIV, but the effect of cART on ADP responses has not been studied previously. Therefore, we compared ADP for serum-purified IgG obtained from all 49 subject at baseline and 96 weeks after cART initiation. We used a modified ADP assay, which allows the specific analyses of internalized (phagocytosed) beads. Figure 3*A* shows the gating strategy for samples obtained before and after cART initiation. This assay distinguishes internalized beads by using FITC- and Cy5-labeled fluorescent internalization probe double-labeled beads. The percentage phagocytosis is determined as the percentage of FITC<sup>+</sup>Cy5<sup>+</sup> monocytes. A small but significant reduction in mean ADP ( $\pm$ SEM) was observed in IgG from serum in the ADP assay between week 0 ( $24.3\% \pm 0.9\%$ ) and week 96 after cART initiation ( $22.5\% \pm 0.9\%$ ;  $P = .018$ ; Figure 3*B*).

### Changes in Fc $\gamma$ R Expression on Monocytes Following Long-term cART

We found decreased ADP and ADCC-mediating Abs in serum samples from donors following prolonged cART, using a monocyte cell line as the effector cell in the ADP assay and either a T-cell line or healthy donor PBMCs in the ADCC assays. However, it is also possible that effector cells such as monocytes from the subjects display changes in frequencies and/or surface expression markers, including Fc $\gamma$ R expression, after prolonged cART, which could compensate for lower levels of effector Abs. We therefore obtained frozen PBMCs obtained at baseline and after

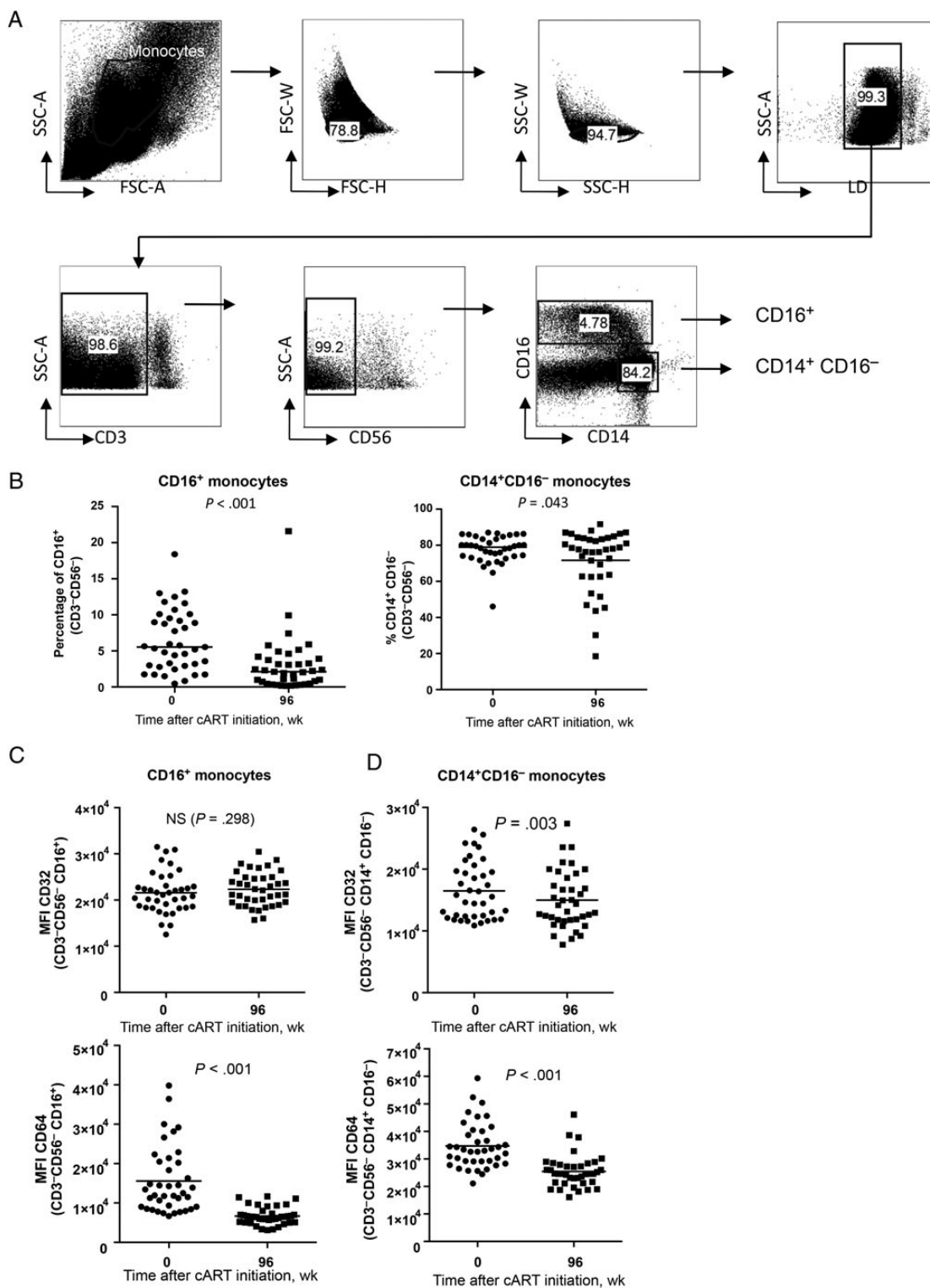


**Figure 4.** Changes in Fc $\gamma$ R expression on monocytes following long-term combination antiretroviral therapy (cART). *A*, Gating on monocytes in the forward and side scatter (FSC/SSC), followed by the exclusion of singlets. Live cells were gated followed by gating on CD3 $^{-}$  and CD56 $^{-}$  cells. The following monocyte subpopulations were selected in CD16 vs CD14 plot: (1) CD16 $^{+}$  (CD14 variable) and (2) CD14 $^{+}$ CD16 $^{-}$  as shown in the plot. Within these 2 gates, total cell frequency and Fc $\gamma$ R expression were analyzed. *B*, Distribution of the frequency of the 2 different subpopulations (39 peripheral blood mononuclear cell samples that had a viability of >85%) comparing week 0 and week 96. Comparisons were made using paired *t* tests. Lines in the graph represent mean bars. *C*, The mean fluorescence intensity (MFI) for CD32 (top panel) and CD64 $^{+}$  (bottom panel) expression within the CD16 $^{+}$  (CD14 variable) monocyte population at weeks 0 and 96. Comparisons were made using paired *t* tests. Lines in the graph represent mean bars. *D*, The MFI for CD32 (top panel) and CD64 (bottom panel) expression within the CD14 $^{+}$ CD16 $^{-}$  monocyte subpopulation, comparing weeks 0 and 96. Comparisons were made using paired *t* tests. Lines in the graph represent mean bars.

96 weeks of cART and evaluated gated monocyte subsets and Fc $\gamma$ R expression on monocytes. Figure 4A shows the gating strategy for selecting the CD16<sup>+</sup> (CD14 variable) and CD14<sup>+</sup>CD16<sup>-</sup> monocyte subpopulations out of gated monocytes where the CD3<sup>+</sup> and CD56<sup>+</sup> cells were excluded. PBMC samples from 39 subjects were analyzed since 10 PBMC samples had viability of <85% and were therefore excluded. When gated on CD16<sup>+</sup> (CD14 variable) monocytes, we observed a significant decrease in the mean percentage ( $\pm$ SEM) of CD16<sup>+</sup> monocytes among the total monocyte population, as shown in Figure 4A, from week 0 (6.4%  $\pm$  0.7%) to week 96 after cART initiation (2.9%  $\pm$  0.6%;  $P < .001$ ; Figure 4B). There was also a significant decrease in the mean percentage ( $\pm$ SEM) of CD14<sup>+</sup>CD16<sup>-</sup> monocytes among the total gated monocyte population from week 0 (77.6%  $\pm$  1.0%) to week 96 (71.6%  $\pm$  2.8%;  $P = .043$ ; Figure 4B).

We then analyzed levels of the other major Fc receptors expressed on monocytes (CD32 and CD64). The mean fluorescence intensity (MFI;  $\pm$ SEM) of CD32 surface expression on the CD16<sup>+</sup> (CD14 variable) monocyte subpopulation did not change from week 0 (21 569  $\pm$  711 units) to week 96 (22 331  $\pm$  584 units;  $P = .298$ ; Figure 4C). However, a significant decrease in mean ( $\pm$ SEM) surface expression of CD64 on monocytes occurred from week 0 (15 593  $\pm$  1349 units) to week 96 (666  $\pm$  351 units;  $P < .001$ ; Figure 4C). Within CD14<sup>+</sup>CD16<sup>-</sup> monocytes, there was a small but significant decrease in the MFI of CD32 ( $P = .003$ ) and a larger decrease in the CD64 MFI ( $P < .001$ ) from week 0 to 96 (Figure 4D).

## DISCUSSION

The introduction of cART has dramatically improved the life expectancy of HIV-infected individuals but comes at a cost of decreased HIV-specific immunity. Reductions in HIV-specific CTLs, as well as total anti-HIV and neutralizing Ab responses, following cART have been reported previously [7, 11–13]. However, the effect of cART on nonneutralizing Ab responses remains unclear. This study provides a rigorous analysis of the effect of cART on the HIV-specific Fc-mediated Ab functionalities of ADCC and ADP. We observed that, in subjects receiving cART, the ADCC and ADP responses declined within 96 weeks. We found consistent decline in ADCC Ab functionality in both the ability of ADCC Abs to kill gp140-coated target cells (in the rapid fluorometric ADCC assay), as well as the ability of ADCC Abs to activate NK cells (in the NK activation ADCC assay). Our data show that virus-specific effector Ab responses diminish with prolonged suppression of viral replication.

In our longitudinal studies of ADCC Ab-mediated killing, we found that the major drop in ADCC occurred after 2 years of cART. We speculate that subsequent years of cART may result in a further decline in HIV-specific ADCC Ab levels.

Recent studies from our laboratory have demonstrated that ADP-mediating Abs develop early during infection and that

ADP responses increase over time in the absence of cART [37]. In the present study, we demonstrated a small but significant decrease in HIV-specific ADP after 96 weeks of cART. Whether this ADP Ab decline results in a decrease in phagocytic function in patients remains to be determined. Future studies using autologous monocytes from patients to assess ADP would be beneficial, but no ADP assay is currently available to study this.

Generalized immune activation remains elevated in patients during long-term cART [38]. Immune activation has been suggested to result in premature age-related changes to monocytes and supports the hypothesis that HIV may accelerate the development of age-related diseases [39]. We found a decrease in the inflammatory CD16<sup>+</sup> monocyte population after cART initiation. The pre-cART CD16<sup>+</sup> monocyte levels were thus consistent with findings of higher levels of CD16<sup>+</sup> monocytes in viremic individuals, but not in virologically suppressed individuals, in cross-sectional studies from other groups [39–41]. This inflammatory CD16<sup>+</sup> monocyte population has been associated with aging [42] and HIV-related dementia [43]. We speculate that the decrease in the proportion of CD16<sup>+</sup> monocytes upon treatment observed in our study is a return to a normal level, although significant numbers of PBMCs from uninfected control donors stored in the same manner will need to be tested concurrently in future studies.

HIV infection-related immune activation may also result in alteration of Fc $\gamma$ R expression on monocytes and result in a potential loss of Ab effector function over time. Whether cART can restore the Fc $\gamma$ R-mediated effector function of monocytes has not been reported. For both CD16<sup>+</sup> (CD14 variable) and CD16<sup>-</sup>CD14<sup>+</sup> populations, we detected decreased CD64 expression after 96 weeks of cART. This is in agreement with previous reports showing that CD64 expression is elevated in HIV-infected individuals and is further linked to the disease stage [44, 45]. Within the CD16<sup>+</sup> CD14-variable population but not the CD16<sup>-</sup> monocyte population, we observed a small increase in CD32 after 96 weeks of cART. The modest changes in Fc $\gamma$ R expression in monocytes, overall, are not likely to compensate for the more substantially decreased ADCC and ADP Ab levels.

In conclusion, our longitudinal study shows that HIV-specific Ab responses such as ADCC and ADP significantly decline in HIV-infected subjects receiving cART. This has important implications for therapeutic vaccines and HIV cure studies. ADCC-based therapeutic vaccines and/or modulation of Fc-mediated effector functions may assist in improving immune control of HIV infection in subjects receiving cART and, potentially, in clearing reactivated latently infected cells.

## Notes

**Acknowledgments.** We thank all of the study participants and healthy volunteer blood donors.

**Financial support.** This work was supported by the Australian National Health and Medical Research Council (award 510448).



**Potential conflicts of interest.** All authors: No reported conflicts.

All authors have submitted the ICMJE Form for Disclosure of Potential Conflicts of Interest. Conflicts that the editors consider relevant to the content of the manuscript have been disclosed.

## References

1. Lafeuillade A. Eliminating the HIV reservoir. *Curr HIV/AIDS Rep* **2012**; 9:121–31.
2. Shan L, Siliciano RF. From reactivation of latent HIV-1 to elimination of the latent reservoir: The presence of multiple barriers to viral eradication. *Bioessays* **2013**; 35:544–52.
3. Battegay M, Nuesch R, Hirschel B, Kaufmann GR. Immunological recovery and antiretroviral therapy in HIV-1 infection. *Lancet Infect Dis* **2006**; 6:280–7.
4. Archin NM, Liberty AL, Kashuba AD, et al. Administration of vorinostat disrupts HIV-1 latency in patients on antiretroviral therapy. *Nature* **2012**; 487:482–5.
5. Kent SJ, Reece JC, Petravic J, et al. The search for an HIV cure: tackling latent infection. *Lancet Infect Dis* **2013**; 13:614–21.
6. International AIDS Society Scientific Working Group on HIV Cure. Towards an HIV cure: a global scientific strategy. *Nat Rev Immunol* **2012**; 12:607–14.
7. Casazza JP, Betts MR, Picker LJ, Koup RA. Decay kinetics of human immunodeficiency virus-specific CD8(+) T cells in peripheral blood after initiation of highly active antiretroviral therapy. *J Virol* **2001**; 75:6508–16.
8. Shan L, Deng K, Shroff NS, et al. Stimulation of HIV-1-specific cytolytic T lymphocytes facilitates elimination of latent viral reservoir after virus reactivation. *Immunity* **2012**; 36:491–501.
9. Buchbinder SP, Mehrotra DV, Duerr A, et al. Efficacy assessment of a cell-mediated immunity HIV-1 vaccine (the Step Study): a double-blind, randomised, placebo-controlled, test-of-concept trial. *Lancet* **2008**; 372:1881–93.
10. Gray GE, Allen M, Moodie Z, et al. Safety and efficacy of the HVTN 503/Phambili Study of a clade-B-based HIV-1 vaccine in South Africa: a double-blind, randomised, placebo-controlled test-of-concept phase 2 h study. *Lancet Infect Dis* **2011**; 11:507–15.
11. Notermans DW, de Jong JJ, Goudsmit J, et al. Potent antiretroviral therapy initiates normalization of hypergammaglobulinemia and a decline in HIV type 1-specific antibody responses. *AIDS Res Hum Retroviruses* **2001**; 17:1003–8.
12. Morris L, Binley JM, Clas BA, et al. HIV-1 antigen-specific and -non-specific B cell responses are sensitive to combination antiretroviral therapy. *J Exp Med* **1998**; 188:233–45.
13. Morris MK, Katzenstein DA, Israelski D, Zolopa A, Hendry RM, Hanson CV. Characterization of the HIV-1 specific humoral immune response during highly active antiretroviral therapy (HAART). *J Acquir Immune Defic Syndr* **2001**; 28:405–15.
14. Hütter G, Nowak D, Mossner M, et al. Long-term control of HIV by CCR5 Delta32/Delta32 stem-cell transplantation. *N Engl J Med* **2009**; 360:692–8.
15. Haynes BF, Gilbert PB, McElrath MJ, et al. Immune-correlates analysis of an HIV-1 vaccine efficacy trial. *N Engl J Med* **2012**; 366:1275–86.
16. Tomaras GD, Ferrari G, Shen XY, et al. Vaccine-induced plasma IgA specific for the C1 region of the HIV-1 envelope blocks binding and effector function of IgG. *Proc Natl Acad Sci U S A* **2013**; 110:9019–24.
17. Baum LL, Cassutt KJ, Knigge K, et al. HIV-1 gp120-specific antibody-dependent cell-mediated cytotoxicity correlates with rate of disease progression. *J Immunol* **1996**; 157:2168–73.
18. Gomez-Roman VR, Patterson LJ, Venzon D, et al. Vaccine-elicited antibodies mediate antibody-dependent cellular cytotoxicity correlated with significantly reduced acute viremia in rhesus macaques challenged with SIVmac251. *J Immunol* **2005**; 174:2185–9.
19. Hessel AJ, Hangartner L, Hunter M, et al. Fc receptor but not complement binding is important in antibody protection against HIV. *Nature* **2007**; 449:101–4.
20. Alpert MD, Harvey JD, Lauer WA, et al. ADCC develops over time during persistent infection with live-attenuated SIV and is associated with complete protection against SIVmac251 challenge. *PLoS Pathog* **2012**; 8:e1002890.
21. Huber M, Trkola A. Humoral immunity to HIV-1: neutralization and beyond. *J Intern Med* **2007**; 262:5–25.
22. Dugast AS, Tonelli A, Berger CT, et al. Decreased Fc receptor expression on innate immune cells is associated with impaired antibody-mediated cellular phagocytic activity in chronically HIV-1 infected individuals. *Virology* **2011**; 415:160–7.
23. Barouch DH, Stephenson KE, Borducchi EN, et al. Protective efficacy of a global HIV-1 mosaic vaccine against heterologous SHIV challenges in rhesus monkeys. *Cell* **2013**; 155:531–9.
24. French MA, Tanaskovic S, Law MG, et al. Vaccine-induced IgG2 anti-HIV p24 is associated with control of HIV in patients with a 'high-affinity' FcgammaRIIa genotype. *AIDS* **2010**; 24:1983–90.
25. Hsu DC, Kerr SJ, Iampornsin T, et al. Restoration of CMV-specific CD4T cells with ART occurs early and is greater in those with more advanced immunodeficiency. *PLoS One* **2013**; 8:e77479.
26. Hsu DC, Kerr SJ, Thongpaeng P, et al. Incomplete restoration of Mycobacterium tuberculosis-specific-CD4 T cell responses despite antiretroviral therapy. *J Infect* **2014**; 68:344–54.
27. Center RJ, Wheatley AK, Campbell SM, et al. Induction of HIV-1 subtype B and AE-specific neutralizing antibodies in mice and macaques with DNA prime and recombinant gp140 protein boost regimens. *Vaccine* **2009**; 27:6605–12.
28. Center RJ, Lebowitz J, Leapman RD, Moss B. Promoting trimerization of soluble human immunodeficiency virus type 1 (HIV-1) Env through the use of HIV-1/simian immunodeficiency virus chimeras. *J Virol* **2004**; 78:2265–76.
29. De Rose R, Chea S, Dale CJ, et al. Subtype AE HIV-1 DNA and recombinant Fowlpoxvirus vaccines encoding five shared HIV-1 genes: safety and T cell immunogenicity in macaques. *Vaccine* **2005**; 23:1949–56.
30. Wren L, Parsons MS, Isitman G, et al. Influence of cytokines on HIV-specific antibody-dependent cellular cytotoxicity activation profile of natural killer cells. *PLoS One* **2012**; 7:e38580.
31. Gomez-Roman VR, Florese RH, Patterson LJ, et al. A simplified method for the rapid fluorometric assessment of antibody-dependent cell-mediated cytotoxicity. *J Immunol Methods* **2006**; 308:53–67.
32. Kramski M, Schorcht A, Johnston AP, et al. Role of monocytes in mediating HIV-specific antibody-dependent cellular cytotoxicity. *J Immunol Methods* **2012**; 384:51–61.
33. Stratov I, Chung A, Kent SJ. Robust NK cell-mediated human immunodeficiency virus (HIV)-specific antibody-dependent responses in HIV-infected subjects. *J Virol* **2008**; 82:5450–9.
34. Chung AW, Rollman E, Center RJ, Kent SJ, Stratov I. Rapid degranulation of NK cells following activation by HIV-specific antibodies. *J Immunol* **2009**; 182:1202–10.
35. Ackerman ME, Moldt B, Wyatt RT, et al. A robust, high-throughput assay to determine the phagocytic activity of clinical antibody samples. *J Immunol Methods* **2011**; 366:8–19.
36. Liu H, Johnston AP. A programmable sensor to probe the internalization of proteins and nanoparticles in live cells. *Angew Chem Int Ed In Engl* **2013**; 52:5744–8.
37. Ana-Sosa-Batiz F, Johnston AP, Liu H, et al. HIV-specific antibody-dependent phagocytosis matures during HIV infection. *Immunol Cell Biol* **2014**. doi:10.1038/icb.2014.42.
38. Rajasuriar R, Booth D, Solomon A, et al. Biological determinants of immune reconstitution in HIV-infected patients receiving antiretroviral therapy: the role of interleukin 7 and interleukin 7 receptor  $\alpha$  and microbial translocation. *J Infect Dis* **2010**; 202:1254–64.
39. Hearps AC, Maisa A, Cheng WJ, et al. HIV infection induces age-related changes to monocytes and innate immune activation in young men that persist despite combination antiretroviral therapy. *AIDS* **2012**; 26:843–53.

40. Jaworowski A, Ellery P, Maslin CL, et al. Normal CD16 expression and phagocytosis of *Mycobacterium avium* complex by monocytes from a current cohort of HIV-1-infected patients. *J Infect Dis* **2006**; 193:693–7.
41. Thieblemont N, Weiss L, Sadeghi HM, Estcourt C, Haeffner-Cavaillon N. CD14<sup>low</sup>CD16<sup>high</sup>: a cytokine-producing monocyte subset which expands during human immunodeficiency virus infection. *European J Immunol* **1995**; 25:3418–24.
42. Nyugen J, Agrawal S, Gollapudi S, Gupta S. Impaired Functions of Peripheral Blood Monocyte Subpopulations in Aged Humans. *J Clin Immunol* **2010**; 30:806–13.
43. Pulliam L, Gascon R, Stubblebine M, McGuire D, McGrath MS. Unique monocyte subset in patients with AIDS dementia. *Lancet* **1997**; 349:692–5.
44. Capsoni F, Minonzio F, Ongari AM, et al. Increased expression of IgG Fc receptor type I on neutrophils and monocytes from HIV-infected subjects. *Clin Exp Immunol* **1992**; 90:175–80.
45. Locher C, Vanham G, Kestens L, et al. Expression patterns of Fc gamma receptors, HLA-DR and selected adhesion molecules on monocytes from normal and HIV-infected individuals. *Clin Exp Immunol* **1994**; 98:115–22.